JSS Focus Issue on Semiconductor-Based Sensors

# AlGaN/GaN Heterostructure Based Schottky Diode Sensors with ZnO Nanorods for Environmental Ammonia Monitoring Applications

**Sunwoo Jung,[1,*] Kwang Hyeon Baik,[2] Fan Ren,[3,**] S. J. Pearton,[4,**] and Soohwan Jang[1,z]**

[1]*Department of Chemical Engineering, Dankook University, Yongin 16890, Korea*
[2]*School of Materials Science and Engineering, Hongik University, Jochiwon, Sejong 30016, Korea*
[3]*Department of Chemical Engineering, University of Florida, Gainesville, Florida 32611, USA*
[4]*Department of Materials Science and Engineering, University of Florida, Gainesville, Florida 32611, USA*

AlGaN/GaN heterostructure Schottky diodes with ZnO nanorod functionalization are shown to be capable of detecting $NH_3$ balanced with air at a concentration of ∼0.3 ppm at 25°C and ∼0.1ppm at 300°C. The diodes show reproducible current response to repeated cycling of the $NH_3$ exposure at all temperatures in this range. The diode current at fixed voltage decreased upon exposure to the $NH_3$, which is opposite to what occurs with exposure to hydrogen. This suggests the detection mechanism involves reaction of ammonia with oxygen species on the ZnO nanorods, increasing the negative charge on the interface with AlGaN. The detection sensitivity displayed an activation energy of 0.071 eV and increased monotonically with ammonia concentration at all temperatures, from 3.36% (25°C) to 12.59% (300°C) for 2 ppm at a voltage of 5 V. The diodes could detect ammonia for either polarity applied bias. The absolute current change and sensitivity upon exposure to ammonia increased with measurement temperature.
 [DOI: 10.1149/2.0041807jss]

Manuscript submitted January 10, 2018; revised manuscript received February 26, 2018. Published March 6, 2018. *This paper is part of the JSS Focus Issue on Semiconductor-Based Sensors for Application to Vapors, Chemicals, Biological Species, and Medical Diagnosis.*

There are many applications where sensitive detection and monitoring of ammonia ($NH_3$) emissions from cars, refrigeration equipment and agricultural systems is needed.[1–11] One of the biggest applications is in monitoring emissions of nitrogen oxides ($NO_x$) during the selective catalytic reduction (SCR) process[1,2,6,7,9] in which ammonia is injected to react with $NO_x$ in the presence of a vanadium catalyst to produce nitrogen and water vapor. This mitigates the amount of $NO_x$ released into the atmosphere and reduces the pollution effects (smog and acid rain) associated with these species. This process is one of the most efficient methods (almost 95% removal of the nitrogen oxides) for reducing industrial emissions from boilers, chemical plants, refineries, gasoline and diesel engines and turbines in the power industry.[1,2,6,7,12] The successful implantation of the SCR process depends on having sensitive ammonia detectors to monitor leaks and slipover of the ammonia.[5,7,13] Ammonia is a colorless gas which at sufficient concentrations causes a severe life-threatening irritation to the respiratory tract of humans.

The most common ammonia sensors are based on metal oxides such as ZnO, $TiO_2$, CuO, $SnO_2$, $In_2O_3$ and $WO_3$, either in thin film or nanostructured form.[11–32] Typical sensitivities of these metal oxide sensors are 2–90 for 1–30 ppm of $NH_3$ for temperatures of 25–300°C.[1,10] Even higher temperature detection capability may be needed for $NH_3$ detection, since emission of this gas is mostly related to combustion processes where temperatures may be >500°C. The specific detection of $NH_3$ in combustion and exhaust gases at these high temperatures therefore requires sensors with high selectivity to $NO_2$.[30] AlGaN/GaN high electron mobility transistors (HEMTs) and Schottky diode sensors can also provide an attractive platform for gas sensing.[33–44] When functionalized with either Pt[35,39,40] or ZnO nanorods[42] in the gate region, these structures are capable of ammonia detection at low concentrations (0.1–2 ppm) in the temperature range 25–300°C for oxide functionalization[42] and up to 600°C with Pt functionalization.[35,39,40] These are typically targeted at automotive applications in response to increasingly strict emission standards. The ZnO-functionalized HEMT sensors were completely selective at 25°C for 2 ppm $NH_3$ over $O_2$, $CO_2$, CO, $CH_4$, and $NO_2$ under the same detection conditions as used for the $NH_3$. Halfaya et al.[35] used a Pt catalyst layer in the gate region for NO, $NO_2$ and $NH_3$ exhaust gas sensors for automotive antipollution systems. Using an optimized design allowed for one sensor to detect all three target gases with acceptable sensitivity.[35] The sensitivity of the sensors was optimized at 600°C, with measured sensitivities to 900 ppm NO, 900 ppm $NO_2$ and 15 ppm $NH_3$ of 24%, 38.5% and 33%, respectively, at this temperature.[35] The response times were of the order of 1 min. for all three gases.[35] The inherent high temperature operating capability and chemical stability of these wide bandgap nitride materials make them potential candidates for real-time anti-pollution systems. Chen et al.[40] demonstrated maximum sensing response of 13.1 and 182.7, respectively, for 35 and 10, 000 ppm $NH_3$/air gases using a Pt-AlGaN/GaN HEMT sensor at 150°C. Bishop et al.[41] used BGaN/ GaN superlattices and Pt contacts to selectively detect $NO_2$ against $NH_3$ for concentrations from 4.5 to 450 ppm with current responsivity of 6.7 mA/($cm^2$ × ppm) at 250 °C with a response time of 5 s.

In this paper, we demonstrate that Schottky diodes based on AlGaN/GaN heterostructures and functionalized with ZnO nanorods on the rectifying contact area are also capable of ammonia detection in the range 0.1–2 ppm over the temperature range 25–300°C. The concentration and temperature dependence of $NH_3$ detection sensitivities of ZnO nanorod functionalized AlGaN/GaN Schottky diodes in air backgrounds were measured. The use of the diode structure simplifies the sensor fabrication compared to a HEMT, and we show that the absolute current change upon ammonia exposure increase with measurement temperature.

## Experimental

The AlGaN/GaN heterostructure layer was grown on *c*-plane sapphire substrate by metal organic chemical vapor deposition (MOCVD). The layer structure included an initial 2 μm thick undoped *c*-plane GaN buffer followed by a 25 nm thick unintentionally doped $Al_{0.25}Ga_{0.75}N$ layer. Ohmic contacts on the front face were formed by photoresist lift-off process of e-beam evaporated

*Electrochemical Society Student Member.
**Electrochemical Society Fellow.
[z]E-mail: jangmountain@dankook.ac.kr

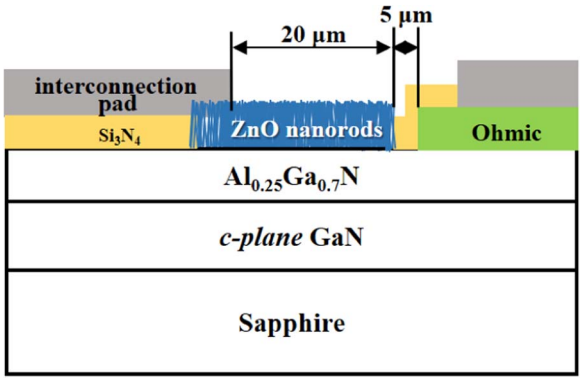


**Figure 1.** Cross-sectional schematic of ZnO-functionalized AlGaN/GaN Schottky diode sensor.

Ti/Al/Ni/Au (25/125/45/100 nm) subsequently annealed at 850°C for 45 s under a flowing $N_2$ ambient in a Heatpulse 610T rapid thermal process system.[44,45] A 200 nm thick plasma-enhanced chemical vapor deposited (PECVD) silicon nitride layer was used for surface passivation.[33,34] Gate area and window region to interconnection pad were patterned by conventional photolithography and etched by buffered oxide etchant for the subsequent ZnO nanorod growth on AlGaN surface and electrical probing of the device. The Schottky contact region of the sensor was functionalized with ZnO nanorods for $NH_3$ sensing.[42,44–46] The ZnO nanorod growth started with preparation of the nano-crystal seeds. The ZnO nano-crystal seed solution was mixed by slowly adding 30 mM NaOH (Sigma–Aldrich) in methanol to a 10 mM zinc acetate dihydrate ($Zn(O_2CCH_3)_2 \cdot 2H_2O$, Sigma–Aldrich) solution at 60°C over 2 hour period. The ZnO nanocrystal seed solution was spun onto the active region of the diode, and the sample was heated at 300°C on a hot plate for 30 minutes in air. The nano-crystalline seed coated diodes were then immersed in an aqueous mixture of 20 mM zinc nitrate hexahydrate ($Zn(NO_3)_2 \cdot 6H_2O$, Sigma–Aldrich) and 20 mM hexamethylenetetramine ($C_6H_{12}N_4$, Sigma–Aldrich) and put in the oven at 94°C for 3 hours for the ZnO nanorod growth. After the nanorod growth, the device was removed from the solution, thoroughly rinsed with deionized water to remove any residual salts, and dried with nitrogen gas. Photoresist was used to pattern the gate area, and dilute HCl solution (1:10 in HCl to $H_2O$ volume ratio) was used to etch off the rest of ZnO nanorods around the gate region.[44,45] Interconnection contacts were formed by the lift-off of e-beam deposited Ti/Au (20/100 nm). A schematic of the final diode sensor is shown in Figure 1.

The completed diodes were exposed to controlled concentrations of $NH_3$ balanced with synthetic air in a test chamber in which mass flow controllers controlled the gas flow rate and injection time. The sensors were mounted on a probe stage in the chamber with electrical feed-throughs connected to an Agilent 4155C parameter analyzer.[47–49] The devices were exposed to $NH_3$ concentrations of 0.1–2 ppm at temperatures from 25 to 300°C. The current-voltage (I-V) characteristics were measured for cycled exposures to different concentrations of the gas at different temperatures.

## Results and Discussion

Figure 2a shows the response of the ZnO nanorod-functionalized diodes to sequential 20 s exposures to 2 ppm humid $NH_3$ in dry air at 25°C, followed by a return to dry air ambient. The applied bias on the diode was 5 V. The same data is shown for exposure at 300°C in Figure 2b. Note that the current decreases upon exposure to the ammonia in both cases and the response is larger at higher temperature. The sensitivity of the sensors is defined as $\frac{I_{air}-I_{NH3}}{I_{air}} \times 100\%$, where $I_{air}$ is the current under an air ambient, and $I_{NH3}$ is the current under the various concentrations of ammonia.[42] As shown in Figure 2c, the sensitivity for 2 ppm detection increased from 3.36% at 25°C to

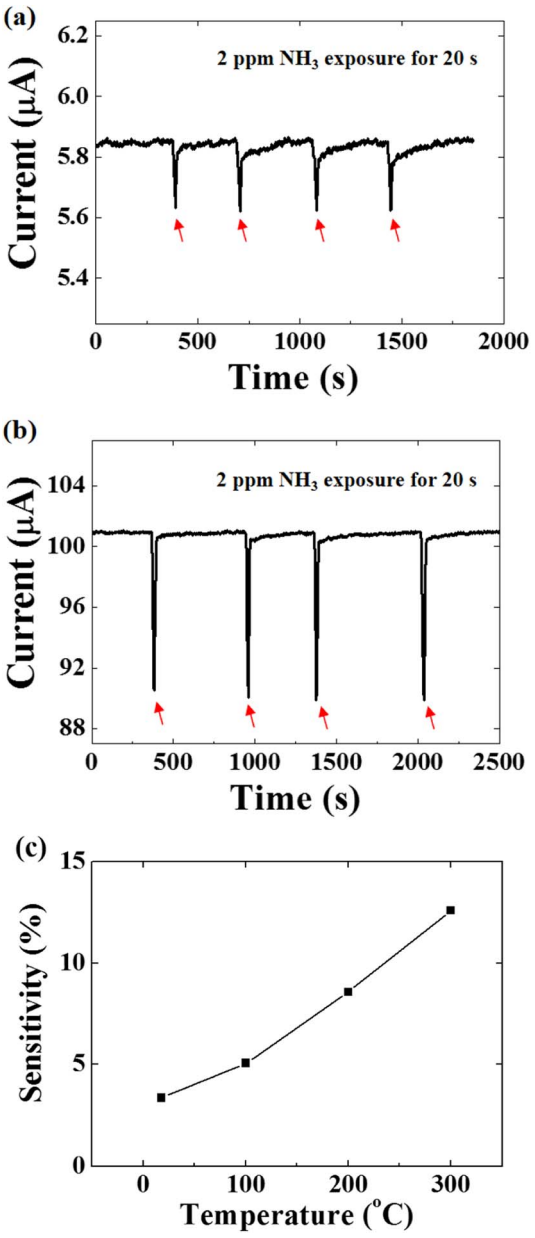


**Figure 2.** Time response of sensors to 20 s sequential exposures of 2 ppm $NH_3$, followed in each case by a return to refreshing air with applied bias of 5 V at (a) 25 and (b) 300°C. (c) sensitivity as a function of temperature for 2 ppm $NH_3$ exposure.

12.59% at 300°C. The response time was defined as the time required to reach 90% of saturated current after 2 ppm ammonia exposure, and the recovery time was defined as the time required to reach 10% of the saturated current after refreshing air exposure. Response times for 2 ppm ammonia exposures at the temperature range of 25–300°C were ~10 s, while the recovery times depended on temperature. The recovery times for 2 ppm ammonia were ~65 and ~10 s for 25 and 300°C, respectively, which are similar to the previously measured ZnO nanorod AlGaN/GaN HEMT sensors.[42]

Figure 3 shows similar time response data for exposure of the sensors to different concentrations (0.1–2 ppm) of humid $NH_3$ in dry air at either (a) 25°C or (b) 300°C. At 25°C, the minimum reliable detection was for a concentration of ~0.3 ppm, while at 300°C, it was possible to detect 0.1 ppm reproducibly. Note that the diode current reverts to a stable level after each repeated exposure, indicating that the ZnO nanorods provide a reproducible platform for transfer of charge

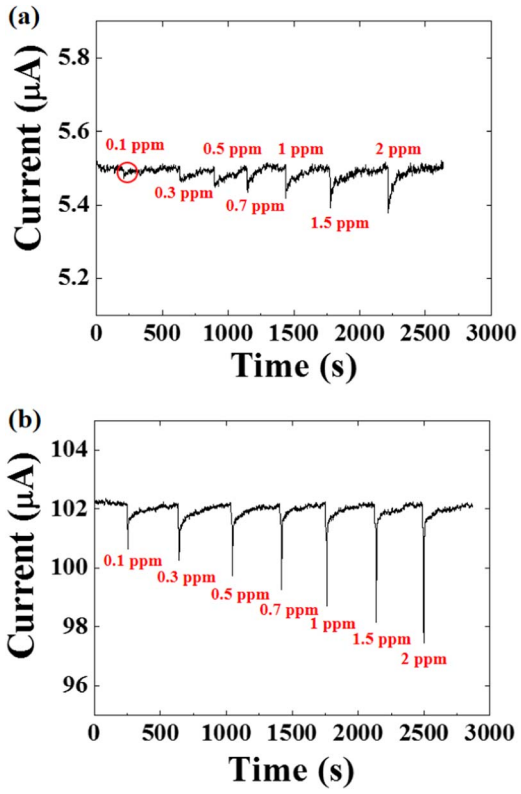


**Figure 3.** Time response of sensors to 20 s sequential exposures of 0.1–2 ppm $NH_3$ followed in each case by a return to refreshing air with applied bias of 5 V at (a) 25 and (b) 300°C.

from the reaction of the adsorbed gas species to the AlGaN/GaN diode.

Figure 4 shows the diode I-V characteristics at four different temperatures (25, 100, 200 and 300°C) in either air or 2 ppm $NH_3$. This again shows the diode current decreases upon exposure to ammonia, which is opposite to the change when detecting reducing gases like hydrogen.[33,34,39,40] For hydrogen detection, we observe the detection mechanism involves an increase in positive charge at the heterointerface that creates the two-dimensional electron gas (2DEG).[33,34,38–40] The charges in the 2DEG at the AlGaN/GaN interface are induced by spontaneous and piezoelectric polarization, which are balanced with positive charges on the surface. The induced sheet carrier concentration of undoped Ga-face AlGaN/GaN can be calculated from[50]

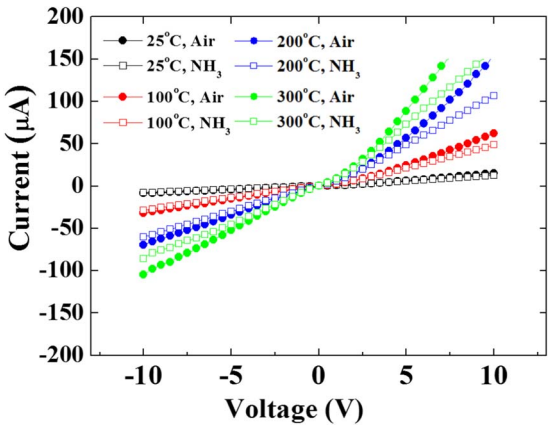


**Figure 4.** Schottky diode sensor I-V characteristics measured in air or 2 ppm $NH_3$ at 25, 100, 200, and 300°C.

$$n_s(x) = \frac{\sigma(x)}{e} - \left(\frac{\varepsilon_0 \varepsilon(x)}{d_d e^2}\right)(e\phi_b(x) + E_F(x) - \Delta E_C(x)) \quad [1]$$

where $\varepsilon_0$ is the electric permittivity, $\varepsilon(x)$ is the relative permittivity, x is the Al mole fraction of $Al_xGa_{1-x}N$, $d_d$ is the AlGaN layer thickness, $e\Phi_b$ is the Schottky barrier of the gate contact on AlGaN, $E_F$ is the Fermi level and $\Delta Ec$ is the conduction band discontinuity between AlGaN and GaN. Therefore, the sheet charge density in the 2D channel of AlGaN/GaN structure is extremely sensitive to its ambient. The adsorption of polar molecules on the surface of AlGaN affects the surface potential and resulting device characteristics. In the case of hydrogen adsorption on a catalytic Schottky metal like Pt, in the gate region, the subsequent decomposition of the hydrogen molecules to atomic hydrogen leads to a change in the effective positive gate surface charges (smaller barrier height, $e\Phi_b$), thereby enhancing the 2DEG density and increasing diode current.[33,38-40] In the present case of $NH_3$ detection, the 2DEG current decreases upon exposure to the gas, suggesting that there is an increase in negative charge at the heterointerface. The mechanism of ammonia reacting with the ZnO nanorods may involve adsorption of oxygen that is reduced by electrons in the n-type ZnO,[7] leading to the reaction $2NH_3 + 3O^-_{ads} \leftrightarrow 3H_2O + N_2 + 3e^-$.[42] The ZnO nanorods always exhibit n-type conductivity related to oxygen vacancies, and therefore can significantly enhance oxygen molecular adsorption.[7] The oxygen species react with the ammonia to return more electrons to the ZnO surface, resulting in an abrupt change in the conductivity of the sensor and enhancing the gas-sensing properties of the nanorod-functionalized HEMT. The decrease in current was also reported by Halfaya et al.[35] for their Pt-functionalized AlGaN/GaN NO and $NO_2$ sensors, Makato et al.[37] for Pd/ZnO/GaN diode $NO_x$ sensors, and Tilak et al.[38] for their GaN Schottky diode NO sensors. However, it should be pointed out that inhibition of the catalyst or transducer layer may occur under certain conditions of concentration or temperature and may complicate interpretation in the absence of oxygen which prevents the nitrogen-induced inhibition of the catalyst.[51,52] In our case, we always used $NH_3$ with 77% relative humidity as a more realistic gas to sense, and this may have helped avoid some of the complications reported by others.[51]

Figure 5 shows the current change in diodes (a) as a function of time at a fixed voltage of 5 V during an exposure to 2 ppm $NH_3$ at temperatures of 25, 100, 200, and 300°C and (b) the magnitude of this current change for the different temperatures. The trend of increasing current in the diode is opposite to our previous results for HEMT detection of ammonia, where the decrease in current results from a decrease in mobility of electrons in the 2DEG. The absolute changes in current increases with temperature from 0.23 μA at 25°C to 10.59 μA at 300°C. By sharp contrast, the HEMT sensors showed an almost constant absolute current change of 60 μA across this temperature range for the same concentration of $NH_3$ (2 ppm). Although both the ZnO nanorod functionalized diode and HEMT show a similar range of sensitivity, the dependence of background current level and absolute current change at different temperatures is an important factor to be considered in real-world sensor applications. Figure 6 shows the percentage sensitivity of the diode sensors as a function of applied voltage at different temperatures. The sensitivity was generally higher at higher bias voltages. Since both forward and reverse bias currents change upon $NH_3$ exposure, either of these modes can be used and the choice of voltage may be determined by power consumption considerations. Figure 7 shows an Arrhenius plot of sensitivity, leading to an activation energy of 0.071 eV for ammonia sensing with the ZnO nanorod-functionalized Schottky diodes. This represents the energy of the rate-limiting step in the formation of a charge depletion layer on the surface of the ZnO due to electron trapping on adsorbed oxygen species and the transfer of the negative charge to the AlGaN surface from the reaction discussed earlier.[5,7]

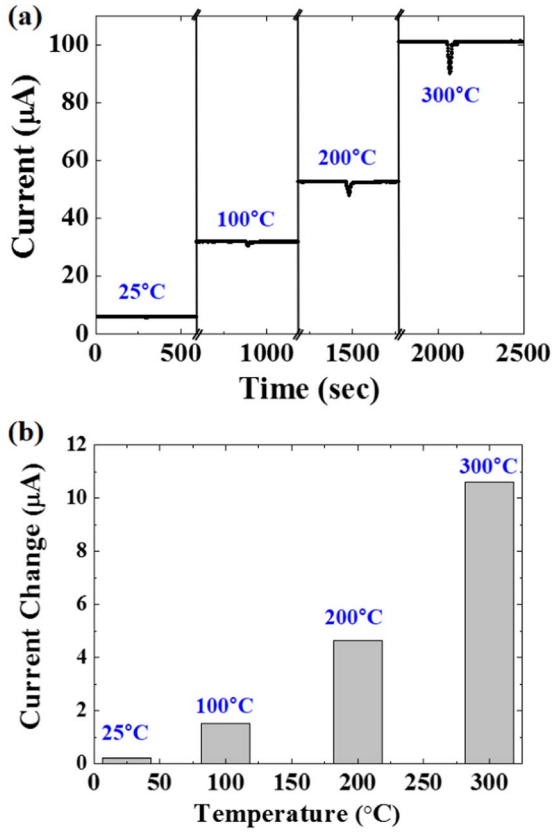


**Figure 5.** Current change in diodes (a) as a function of time at a fixed voltage of 5 V during an exposure to 2 ppm $NH_3$ at temperatures of 25, 100, 200, and 300°C and (b) magnitude of this current change for the different temperatures.

## Conclusions

ZnO-nanorod-functionalized AlGaN/GaN Schottky diode sensors detected low concentrations (0.1–2 ppm) of ammonia at temperatures in the range 25–300°C. In contrast to AlGaN/GaN heterostructure hydrogen sensors functionalized with Pt, the diode current decreased upon ammonia exposure. The mechanism is not due to the diffusion of dissociated hydrogen from $NH_3$ to the heterointerface, since the barrier height and current change show the opposite sign upon exposure to ammonia versus that with hydrogen. The absolute current change and sensitivity for ammonia exposure increased with measurement temperature, and the response time and recovery time were ∼10 s and 10–65 s at 25–300°C respectively. The simple fabrication and excellent thermal stability of the ZnO/AlGaN/GaN diodes indicates these have potential for applications like automobile exhaust sensing.

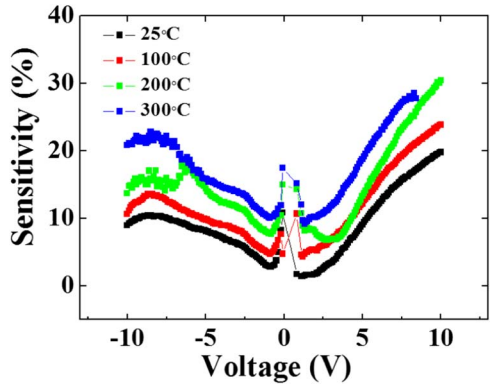


**Figure 6.** Percentage sensitivity of diode sensors as a function of applied voltage at different temperatures.

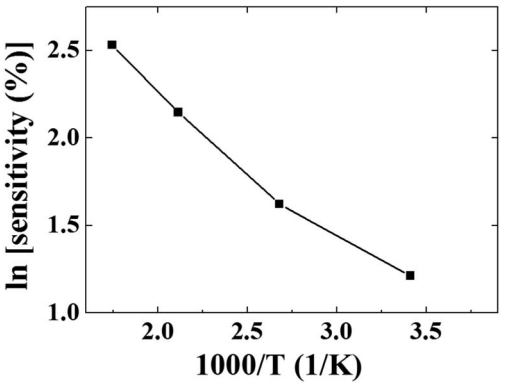


**Figure 7.** Arrhenius plot of sensitivity to detection of 2 ppm $NH_3$ at an applied voltage of 5 V.

## Acknowledgments

This research was supported by the Basic Science Research Program through the National Research Foundation of Korea (NRF) funded by the Ministry of Education (2015R1D1A1A01058663, 2017R1D1A3B03035420), and Nano Material Technology Development Program through the National Research Foundation of Korea (NRF) funded by the Ministry of Science, ICT and Future Planning (2015M3A7B7045185). The work at UF was partially supported by HDTRA1-17-1-001.

## ORCID

Fan Ren https://orcid.org/0000-0001-9234-019X
S. J. Pearton https://orcid.org/0000-0001-6498-1256
Soohwan Jang https://orcid.org/0000-0002-8188-6274

## References

1. P. Guo and H. Pan, *Sens. Actuators, B*, **114**, 762 (2006).
2. E. Bekyarova, M. Davis, T. Burch, M. E. Itkis, B. Zhao, S. Sushine, and R. C. Haddon, *J. Phys. Chem. B*, **108**, 19717 (2004).
3. N. H. Quang, M. V. Trinh, B. Lee, and J. Huh, *Sens. Actuators, B*, **113**, 341 (2006).
4. F. V. Paez, A. H. Romero, E. M. Sandoval, L. M. Martinez, H. Terrones, and M. Terrones, *Chem. Phys. Lett.*, **386**, 137 (2004).
5. C. S. Rout, M. Hegde, A. Govindaraj, and C. N. R. Rao, *Nanotechnology*, **18**, 205504 (2007).
6. M. S. Wagh, G. H. Jain, D. R. Patil, S. A. Patil, and L. A. Patil, *Sens. Actuators, B*, **115**, 128 (2006).
7. B. Timmer, W. Olthuis, and A. Berg, *Sens. Actuators, B*, **107**, 666 (2005).
8. M. Aslam, V. A. Chaudhary, I. S. Mulla, S. R. Sainkar, A. B. Mandale, A. A. Belhekar, and K. Vijayamohanan, *Sens. Actuators, A*, **75**, 162 (1999).
9. Y. Wang, X. Wu, Q. Su, Y. Li, and Z. Zhou, *Solid-State Electron.*, **45**, 347 (2001).
10. C. S. Rout, A. Govindaraj, and C. N. R. Rao, *J. Mater. Chem.*, **16**, 3936 (2006).
11. C. S. Rout, S. H. Krishna, S. R. C. Vivekchand, A. Govindaraj, and C. N. R. Rao, *Chem. Phys. Lett.*, **418**, 586 (2006).
12. I. Jiménez, J. Arbiol, A. Cornet, and J. R. Morante, *IEEE Sens. J.*, **2**, 329 (2002).
13. B. Marquis and J. Vetelino, *Sens. Actuators, B*, **77**, 100 (2001).
14. J. Samà, S. Barth, G. Domènech-Gil, J. D. Prades, N. López, O. Casals, I. Gràcia, C. Cané, and A. Romano-Rodríguez, *Sens. Actuators, B*, **232**, 402 (2016).
15. J. M. Tulliani, A. Cavalieri, S. Musso, E. Sardella, and F. Geobaldo, *Sens. Actuators, B*, **152**, 144 (2011).
16. A. G. Bannov, J. Prášek, O. Jašek, A. A. Shibaev, and L. Zajíčková, *Procedia Eng.*, **168**, 231 (2016).
17. D. Zhang, C. Jiang, and Y. Sun, *J. Alloys Compd.*, **698**, 476 (2017).
18. S. Han, X. Zhuang, Y. Jiang, X. Yang, L. Li, and J. Yu, *Sens. Actuators, B*, **243**, 1248 (2017).
19. R. H. Vignesh, K. V. Sankar, S. Amaresh, Y. S. Lee, and R. K. Selvan, *Sens. Actuators, B*, **220**, 50 (2015).
20. B. Chatterjee and A. Bandyopadhyay, *Environ. Qual. Manage.*, **26**, 89 (2016).
21. F. Rigoni, S. Tognolini, P. Borghetti, G. Drera, S. Pagliara, A. Goldoni, and L. Sangaletti, *Procedia Eng.*, **87**, 716 (2014).

22. D. A. Burgard, T. R. Dalton, G. A. Bishop, J. R. Starkey, and D. H. Stedman, *Rev. Sci. Instrum.*, **77**, 014101 (2006).
23. M. Gautam and A. H. Jayatissa, *J. Appl. Phys.*, **111**, 094317 (2012).
24. X. Wang, J. Zhang, and Z. Zhu, *Appl. Surf. Sci.*, **252**, 2404 (2006).
25. V. B. Raj, A. T. Nimal, Y. Parmar, M. U. Sharma, and V. Gupta, *Sens. Actuators, B*, **166**, 576 (2012).
26. G. S. T. Rao and D. T. Rao, *Sens. Actuators, B*, **55**, 166 (1999).
27. Y. L. Tang, Z. J. Li, J. Y. Ma, Y. J. Guo, Y. Q. Fu, and X. T. Zu, *Sens. Actuators, B*, **201**, 114 (2014).
28. I-Cherng Chen, Shiu-Shiung Lin, Tsao-Jen Lin, Cheng-Liang Hsu, Ting Jen Hsueh, and Tien-Yu Shieh, *Sensors* **10**, 3057(2010).
29. Kang-Min Kim, Hyun-Mook Jeong, Hae-Ryong Kim, Kwon-Il Choi, Hyo-Joong Kim, and Jong-Heun Lee, *Sensors* **12**, 8013 (2012).
30. B. Saruhan, A. A. Haidry, A. Yüce, E. Ciftyürek, and G. C. M. Rodríguez, *Chemosensors* **4**, 8 (2016).
31. F. Schútt, V. Postica, R. Adelung, and O. Lupan, *ACS Appl. Mater. Interfaces* **9**, 23107 (2017).
32. V. Postica, F. Schütt, R. Adelung, and O. Lupan, *Adv. Mater. Interfaces* **4**, 1700507 (2017).
33. S. J. Pearton, B. S. Kang, S. Kim, F. Ren, B. P. Gila, C. R. Abernathy, Jenshan Lin, and S. N. G Chu, *J Physics: Condensed Matter* **16**, R961 (2004).
34. S. J. Pearton, F. Ren, Yu-Lin Wang, B. H. Chu, K. H. Chen, C. Y. Chang, Wantae Lim, Jenshan Lin, and D. P. Norton, *Prog. Mat. Sci.* **55**,1 (2010).
35. Y. Halfaya, C. Bishop, A. Soltani, S. Sundaram, V. Aubry, P. L. Voss, J.-P. Salvestrini, and A. Ougazzaden, *Sensors* **16**,273(2016).
36. H. I. Chen, C. S. Hsu, C. C. Huang, C. F. Chang, P. C. Chou, and W. C. Liu, *IEEE Electron. Device Lett.* **33**, 612 (2012).
37. M. Makoto, F. Shu, and E. Takashi, *J. Vac. Sci. Technol.* **33**, 013001(2015).
38. V. Tilak, K. Matocha, and P. Sandvik, *Phys. Status Solidi* **7**, 2555 (2005).
39. J. Schalwig, G. Muller, M. Eickhoff, O. Ambacher, and M. Stutzmann, *Mater. Sci. Eng. B* **93**, 207 (2002).
40. H. I. Chen, Y. J. Liu, C. C. Huang, C.-S. Hsu, C.-F. Chang, and W. F. Liu, *Sens. Actuators B Chem.* **45**, 347 (2011).
41. C. Bishop, J. P. Salvestrini, Y. Halfaya, S. Sundaram, Y. el Gmili, L. Pradere, J. Y. Marteau, M. B. Assouar, P. L. Voss, and A. Ougazzaden, *Appl. Phys. Lett.* **106**, 243504 (2015).
42. Sunwoo Jung, Kwang Hyeon Baik, F. Ren, S. J. Pearton, and Soohwan Jang, *J. Vac. Sci. Technol. B* **35**, 042201 (2017).
43. X. Jia, D. Chen, L. Bin, H. Lu, R. Zhang, and Y. Zheng, *Sci. Rep.*, **6**, 27728 (2015).
44. S. C. Hung, W. Y. Woon, F. Ren, and S. J. Pearton, *Appl. Phys. Lett.* **103**, 083506 (2013).
45. C. F. Lo, Y. Xi, L. Liu, S. J. Pearton, S. Doré, C. H. Hsu, A. M. Dabiran, P. P. Chow, and F. Ren, *Sens. Actuators, B*, **176**, 708 (2013).
46. B. S. Kang, H. T. Wang, F. Ren, and S. J. Pearton, *J. Appl. Phys.* **104**, 031101 (2008).
47. S. Jang, J. Kim, and K. H. Baik, *J. Electrochem. Soc.*, **163**, B456 (2016).
48. K. H. Baik, J. Kim, and S. Jang, *ECS Trans.*, **72**, 23 (2016).
49. S. Jang, P. Son, J. Kim, S. Lee, and K. H. Baik, *Sens. Actuators, B*, **222**, 43 (2016).
50. M. S. Shur, *Physics of Semiconductor Devices*, (Prentice Hall, Eaglewood Cliffs, NJ 1990).
51. V. Tilak, K. Matocha, and P. Sandvik, *Phys. Status Solidi C* **3**,548 (2006).
52. J. Despres, M. Elsener, M. Koebel, O. Kröcher, B. Schnyder, and A. Wokaun, *Appl. Catalysis B* **50**, 73 (2004).